Dalton Transactions

PAPER

View Article Online
View Journal | View Issue

Cite this: *Dalton Trans.*, 2018, **47**, 15845

[3]rotaxanes composed of two dibenzo-24-crown-8 ether wheels and an azamacrocyclic complex†‡

Mateusz Woźny, *[a] Agnieszka Więckowska,[b] Damian Trzybiński,[c] Szymon Sutuła,[c] Sławomir Domagała[c] and Krzysztof Woźniak [c]

Received 7th August 2018,
Accepted 9th October 2018

DOI: 10.1039/c8dt03225d

rsc.li/dalton

The azamacrocyclic complex was used as a platform for the construction of [3]rotaxanes containing two DB24C8 macrocycles per molecule. The complex unit incorporates two electron deficient π-bond systems and two N–H hydrogen bond donating groups which facilitated the formation of a 1 : 2 interlocked structure. Synthesis and properties of such compounds are presented. Structures of the obtained compounds were confirmed by NMR spectroscopy, ESI mass spectrometry, elemental analysis and single crystal X-ray diffraction. Both [3]rotaxanes containing two DB24C8 macrocycles per molecule crystallise in $P\bar{1}$ and $P2_1/n$ space groups. They have different counterions (PF_6^- and Cl^- anions, respectively) and mostly disordered solvent molecules such as water, methanol and acetone. Both [3]rotaxanes have a flexible axle in which the Cl^- salt takes the shape closer to the "S"-letter, while in the PF_6^- case the axle is more linear. The shape results from respective packing and intra-, and intermolecular interactions among the moieties in the rotaxane and the crystal lattice.

Introduction

Artificial molecular devices include molecular switches based on mechanically interlocked molecules (MIMs) such as catenanes and rotaxanes.[1–7] These objects of the curiosity-driven research allow us to pursue the vision of applications in materials chemistry, sensors, photonics, catalysis and molecular electronics.[8,9] The pioneering work of Stoddart,[2] Sauvage[3] and Feringa[10] in this area was honoured by the Nobel Prize in Chemistry in 2016.[4]

Our group has constructed several [2]catenanes,[11,12] molecular necklaces,[13] and [2]rotaxanes[14–16] from tetraazamacrocyclic complexes (TAM)[17] and dibenzo-24-crown-8 (DB24C8). DB24C8 is a well-known π-donor macrocycle present in many MIMs containing complementary acceptors, such as 4,4-bipyridinium,[18,19] 1,2-bis(pyridinium)ethane,[20–24] or benz-imidazolium.[25,26] DB24C8 was also widely employed in the synthesis of rotaxanes incorporating dialkylammonium ions hosted in the crown ether cavity by the N^+–H···O interactions, which is manifested by short H···O contacts.[27]

DB24C8 is a workhorse macrocycle in our laboratory as it readily forms pseudorotaxanes with the TAM complexes by engaging both of its interaction modes: π-stacking and N–H···O hydrogen bonding. In the DB24C8/TAM pair, the complex unit is a π-acceptor and a hydrogen bond donor. Interestingly, the TAM unit has two electron deficient π-bond systems and two N–H groups bearing a partial positive charge.[16] Such a double-sided structure suggests that simultaneous interaction of the TAM unit with two DB24C8 rings is, at least, in principle possible. However, all MIMs obtained by us so far were characterized by the $(TAM)_2$·DB24C8 composition, corresponding to one DB24C8 macrocycle enclosed between two linked TAMs.[11–16]

The occurrence of a herein suggested, hypothetical TAM·$(DB24C8)_2$ motif, *e.g.* [3]rotaxane composed of a TAM complex and two DB24C8 rings, has never been observed, although there are many examples of [3]rotaxanes described in the literature.[28–33] However, none of them is TAM-based and only some incorporate DB24C8.[34–39] Therefore, we have decided to investigate whether it is possible for the TAM complex to interact with two DB24C8 rings.

In this paper, a synthetic method deliberately aiming at [3]rotaxanes with the TAM·$(DB24C8)_2$ composition is proposed and showed to be successful. The hydroxyl-terminated TAM·$(DB24C8)_2$ pseudorotaxanes were stoppered in a high yielding isocyanate addition. Isocyanates were generated during Curtius rearrangement of corresponding acyl azides. A similar approach involving the reaction between isocyanate

[a]*Institute of Organic Chemistry, Polish Academy of Sciences, Kasprzaka 44/52, 01-224 Warszawa, Poland. E-mail: mateusz.wozny@icho.edu.pl*
[b]*Faculty of Chemistry, University of Warsaw, Pasteura 1, 02-093 Warszawa, Poland*
[c]*Biological and Chemical Research Centre, Chemistry Department, University of Warsaw, Żwirki i Wigury 101, 02-089 Warszawa, Poland*

†Dedicated to Professor Bohdan Korybut-Daszkiewicz on the occasion of his 75th birthday.

‡Electronic supplementary information (ESI) available: NMR spectra, X-ray crystallographic information, and additional voltammetric data. CCDC 1856147 and 1856148. For ESI and crystallographic data in CIF or other electronic format see DOI: 10.1039/c8dt03225d

and amine or the hydroxyl groups was successfully applied to the synthesis of MIMs also in the past.[40–44]

Results and discussion

Synthesis and spectroscopic studies

Compound **1**, obtained according to the new one-pot synthetic protocol,[45] was *O*-methylated with methyl trifluoromethanesulfonate and then treated with 4-amino-1-butanol to give complex **2** with a satisfactory yield (Scheme 1). The hydroxyl end groups in **2** allowed us to employ fast and high yielding isocytanate-to-hydroxyl addition at the stoppering step. In reactions between **2** and 3,5-dinitro- (**3n**) or 3,5-methoxybenzoyl isocyanate (**3m**), we obtained "bare axles" **4n** and **4m** (Scheme 1). Isocyanates **3** were generated in the reaction flask prior to the addition of the complex **2**, *via* thermal Curtius rearrangement of the corresponding acyl azides. The 3,5-dinitro- and 3,5-methoxybenzoyl azides were synthesized from benzoyl chlorides and NaN_3 (yields 80% and 91%, respectively). The azides are easy to purify, handle and store, and can be treated as a protected form of the isocyanates.

In principle, the diol **2** is an appropriate substrate for [3]pseudorotaxane synthesis, since its molecule incorporates two electron deficient π-bond systems and two hydrogen-bond-donating N–H groups. In reactions between **2** and isocyanates **3**, carried out in the presence of an excess of DB24C8, we obtained a series of mechanically interlocked molecules (Scheme 2). [2]rotaxanes **5n** (28%) and **5m** (24%) were the main products, but a substantial amount of target [3]rotaxanes was also obtained – **6n** (16%) and **6m** (13%). This result proves that simultaneous interaction of the TAM complex unit with two DB24C8 macrocycles is factual.

Synthesis of rotaxanes from complex **2**, DB24C8 and acyl azides, carried out under high-temperature conditions in which the Curtius rearrangement occurs *in situ*, is also possible but less efficient. The reaction performed in refluxing acetonitrile gave rotaxanes **5m** and **6m** in 17% and 8% yields, respectively. The difference in yields between the high- and room-temperature reactions can be explained by a lower equilibrium concentration of the pseudorotaxane at higher temperatures. This is in accordance with ^{1}H NMR spectra measurements of a mixture of **4n** and DB24C8, suggesting that the amount of pseudorotaxanes in dynamic equilibrium falls with the temperature increase (Fig. 19S and 20S (ESI‡)).

Structures of the obtained compounds were confirmed by NMR spectroscopy (^{1}H, ^{13}C, HSQC, ROESY; Fig. 1S–16S (ESI‡)), mass spectrometry and elemental analysis. A comparison of NMR spectra of an axle **4n**, [2]rotaxane **5n**, and [3]rotaxane **6n** (Fig. 1) showed changes in shapes and chemical shifts of ^{1}H signals of the TAM unit, occurring upon threading of DB24C8 wheels.

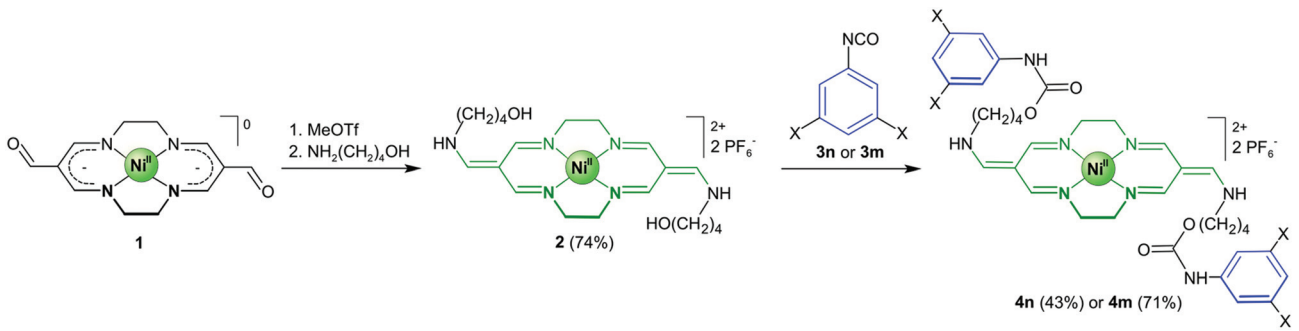

Scheme 1 Synthesis of the substrate for rotaxanes (complex **2**) and its reaction with 3,5-dinitro (**3n**) or 3,5-dimethoxy isocyanate (**3m**), giving bare axles **4n** and **4m**. Isocyanates **3** were generated in the reaction flask, through Curtius rearrangement of corresponding acyl azides, prior to the addition of the complex **2**.

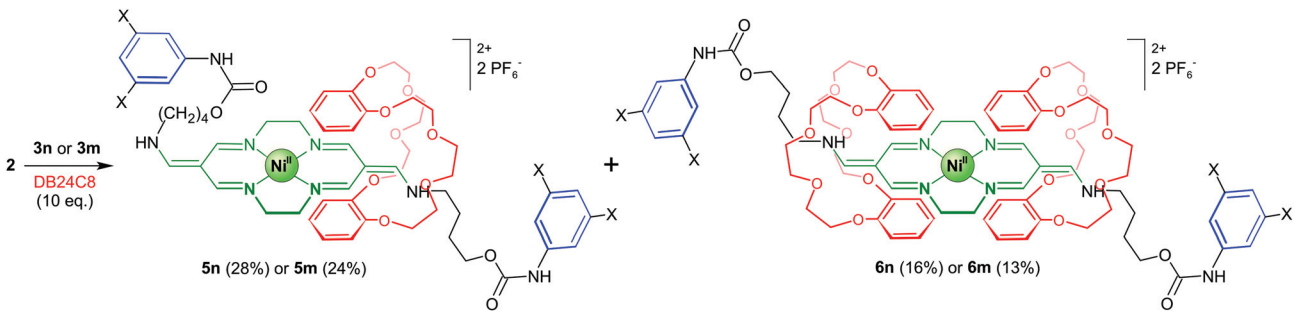

Scheme 2 Threading-stoppering synthesis of [2]- and [3]rotaxanes based on DB24C8 and tetraazamacrocyclic complex. The first TAM-based [3]rotaxanes (**6n** and **6m**) are formed alongside [2]rotaxanes (**5n** and **5m**). Fast and high-yielding isocyanate-to-hydroxyl addition plays a role of the stoppering reaction.

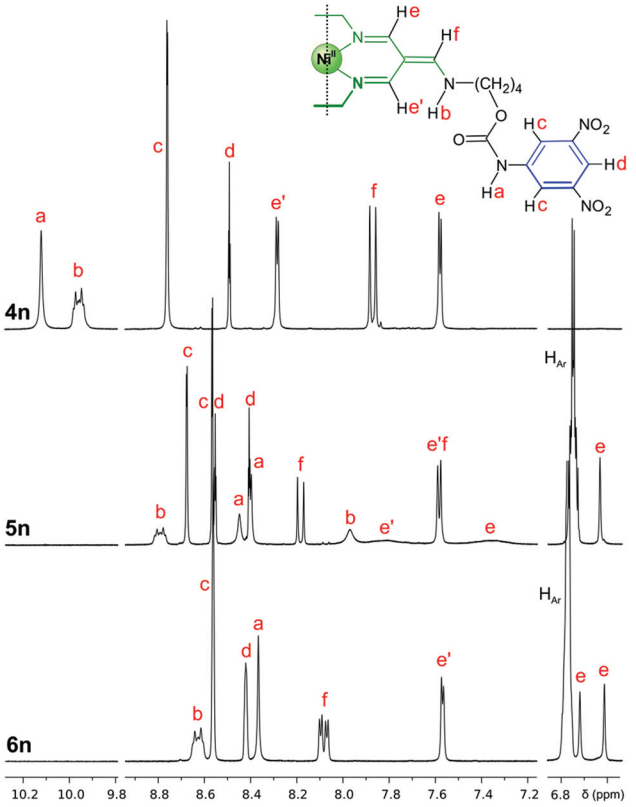

Fig. 1 Low field fragments of the ^{1}H NMR spectra of axle **4n**, [2]rotaxane **5n** and [3]rotaxane **6n** (600 MHz, CD_3CN, 25 °C). H_{Ar} denote protons in aromatic rings of DB24C8.

In the spectrum of **4n**, both acidic NH groups of protons, **a** ($NHCO_2$) and **b** (NH–CH=), appear at low field (10.12 and 9.69 ppm). Protons **b** are coupled to protons **f** (7.87 ppm, NH–CH=), with a vicinal *trans* coupling constant: J = 15.6 Hz. Protons **b** are characterized by an unusually high value of the chemical shift (9.69 ppm), compared with other known TAM complexes. This effect can be explained by the existence of hydrogen bonds between protons **b** and the carbamate group. The interaction causes protons **b** not to exchange chemically and the signal retains its subtle structure.

Signals of imine protons **e** appear at 7.57 and 7.58 ppm, while **e′** at 8.23 and 8.29 ppm (^{1}H nuclei closer to the N atom). Splitting of **e** and **e′** signals results from the existence of two isomers of **4n** in the solution: *cis* and *trans*, differing in the spatial relationship of the two substituents of the macrocyclic ligand. This observation means that the rotation of both exocyclic C=C bonds in axle **4n** is slow in the NMR time-scale.

[2]rotaxane **5n** is composed of an axle **4n** and one DB24C8 macrocycle. A large signal coming from protons attached to the catechol rings of DB24C8 appears at 6.75 ppm. As a whole, the spectrum of **5n** is more complex than in the case of **4n** because of the lower symmetry of the molecule.

Signals **a** appear at 8.40 and 8.45 ppm. The latter one, corresponding to the carbamate group on the side that is not threaded through the DB24C8 wheel, is broad due to chemical exchange. Similarly, proton **b** distant from DB24C8 (7.97 ppm) does not engage in hydrogen bonding, but undergoes exchange as evidenced by signal broadening and the presence of chemical exchange correlations in the ROESY spectrum (Fig. 7S (ESI‡)). A chemical shift of 7.97 ppm is characteristic of NH groups in TAM complexes. On the other hand, the signal of proton **b** located on the side threaded through DB24C8 is pushed towards a lower field (~8.8 ppm). This observation can be explained by the fact that the proton in this NH group engaged in N–H···O hydrogen bonding with the crown ether. Additionally, interaction with DB24C8 freezes chemical exchange and signal **b** appears as a multiplet coupled to proton **f** (doublet at 8.18 ppm, J = 16.2 Hz).

In the spectra of [2]rotaxane **5n**, significant changes in nature and chemical shifts of imine protons **e** and **e′** can also be observed. Indeed, threading an axle through the wheel changes electronic relationships in the complex molecule. Protons distant from DB24C8 appear as two very broad signals at ~7.4 and ~7.8 ppm. The broadening of peaks can be explained by relatively fast rotation of the whole $ArNHCO_2(CH_2)_4NHCH$ = substituent of the ligand, around the exocyclic C=C double bond (different extent of broadening of the signals **e**/**e′** and **b** within the same substituent results from being caused by different dynamic processes). On the DB24C8 side, however, the rotation is hindered by interaction with the crown ether, and signals **e** and **e′** appear as sharp singlets at 6.63 and 7.59 ppm, respectively. An exceptionally low frequency of the latter signal results from the shielding by the surrounding benzene rings of DB24C8. This characteristic feature has been observed for all TAM/DB24C8-based rotaxanes known so far.[14,15]

In the ^{1}H NMR spectrum of the [3]rotaxane **6n**, protons **a–d** and **f** (8.34, 8.63, 8.56, 8.42 and 8.08 ppm, respectively) are no longer duplicated, owing to the symmetric structure of the molecule. Hydrogen-bonding protons in NH groups (**b**) are coupled to protons **f** with J = 16.8 Hz. Since two DB24C8 macrocycles are present in the molecule, not one but two signals **e** appear in the spectrum at exceptionally low chemical shifts: 6.72 and 6.61 ppm. This is due to the fact that, similarly to the complex **4n**, [3]rotaxane **6n** exhibits *cis*/*trans* isomerism in the solution, which manifests itself also in the splitting of signals **e′** and **f** (7.57 and 8.08 ppm).

Aromatic protons of dinitroaryl stoppers in **5n** and **6n** are also influenced by DB24C8. In **6n**, doublets **c**, closer to the DB24C8 moiety, shift by 0.20 ppm towards higher field when compared to **c** in **4n**. In the case of more distant protons **d**, the change is less significant (0.07 ppm).

The presence of DB24C8 influences all of the signals of [2]- and [3]rotaxane axles, including these located within the high field fragment of the ^{1}H NMR spectra of **5n** and **6n** (Fig. 5S and 11S (ESI‡)). Similar effects can be observed when spectra of methoxy-substituted compounds **4m**, **5m** and **6m** are compared (Fig. 3S, 8S, and 14S (ESI‡)).

The co-conformational freedom in studied rotaxanes was not observed. NMR data suggest that DB24C8 resides solely on the TAM unit: dinitrobenzene groups in **5n** and **6n** rotate freely

causing signals c to be averaged (Fig. 1); also, there is no ROESY correlation between the wheel and the stoppers (Fig. 7S and 13S (ESI‡)). This is consistent with the below described voltammetric results, as well as with the X-ray data for the rotaxanes in the solid state.

X-ray crystallographic studies

Attempts to obtain single-crystals suitable for X-ray diffraction measurements of all synthesized compounds were undertaken. However, they were successful only in the case of **6n** (hexafluorophosphate salt) and its counterion exchanged congener (**6nCl**, dichloride salt).

Single-crystal X-ray diffraction analysis confirmed the composition of the investigated compounds and both consist of the same [3]rotaxane axle. However, they contain different anions and solvent molecules in their crystal lattices. The **6n** crystallizes in the triclinic $P\bar{1}$ space group with half of the [3]rotaxane cation (the Ni-atom is situated at the inversion centre), one PF_6^- anion and additional solvent molecules used for crystallization (water, methanol and acetone) in the asymmetric part of the unit cell (Fig. 17Sa (ESI‡)). The mentioned solvents are in a non-stoichiometric ratio to the [3]rotaxane moiety. All nitro groups of the [3]rotaxane axle and the PF_6^- counterions are disordered over two positions. In turn, the latter compound (**6nCl**) crystallizes in the monoclinic $P2_1/n$ space group with half of the [3]rotaxane cation (as in the previous case, the Ni-atom is also located at the inversion centre), one chloride anion and one molecule of acetonitrile in the asymmetric part of the unit cell (Fig. 17Sb (ESI‡)). The details of crystallographic data and the refinement parameters are summarized in Table 1. The full list of bond lengths, valence and torsion angles can be found in Tables 1S–6S (ESI‡). The representation of molecular structure of both compounds is presented in Fig. 2.

In the **6nCl**, the conformation of the [3]rotaxane axle is the closest to the "S"-shape, while in **6n** the mentioned moiety is more extended with two phenyl rings of the 3,5-dinitrophenyl substituents separated by a distance of 30.61(2) Å (Table 2). In both compounds, the adjacent dibenzo-24-crown-8 ether wheels are located close to the Ni center of TAM^{2+} unit in a way that aromatic rings denoted by C12–C17 atoms are involved in the Ni···π contacts (Fig. 2, Tables 9S and 12S‡). The position of the crown ethers is also stabilized by the N–H···O and C–H···O hydrogen bonds between the H-atoms of the CH–NH spacers and C–H fragments of the TAM complex and the oxygen atoms of the DB24C8 unit (Fig. 3, Tables 7S and 11S‡). In **6n**, two weak intramolecular C–H···O hydrogen bonds were identified (Fig. 3a and Table 7S‡) whereas in **6nCl** only one interaction of this type is present (Fig. 3b and Table 11S‡).

In the crystal of **6n**, the ionic species and solvent molecules form specific 3D supramolecular architecture (see Fig. 4). Apparently, the positively charged [3]rotaxane moieties form cavities in the crystal lattice which are filled in by disordered anions and solvent molecules. The arrangement of species in the crystal is dominated by the formation of hydrogen bonds (Table 7S‡); however neighboring [3]rotaxane axles participate also in the intermolecular π–π contacts (Table 8S‡ and Fig. 5) involving adjacent aromatic rings of the 3,5-dinitrophenyl substituents. Interestingly, also the PF_6^- counterions are involved in the C–F···π contacts with aforementioned aromatic rings

Table 1 Crystal data and structure refinement details for **6n** and **6nCl**

Identification code	**6n**	**6nCl**
Empirical formula	$C_{87.92}H_{118.26}F_{12}N_{12}NiO_{30.89}P_2$	$C_{86}H_{110}Cl_2N_{14}NiO_{28}$
Formula weight	2186.13	1917.48
Temperature/K	100(2)	100(2)
Crystal system	Triclinic	Monoclinic
Space group	$P\bar{1}$	$P2_1/n$
a/Å	11.7523(3)	12.7551(3)
b/Å	13.4144(3)	22.9462(4)
c/Å	16.3890(4)	16.8432 (4)
α/°	76.0271(19)	90
β/°	89.369(2)	110.074 (2)
γ/°	81.8124(19)	90
Volume/Å^3	2480.98(11)	4630.20 (17)
Z	1	2
ρ_{calc}/g cm^{-3}	1.463	1.375
μ/mm^{-1}	1.529	0.353
F(000)	1143.0	2020.0
Crystal size/mm^3	0.16 × 0.12 × 0.05	0.41 × 0.20 × 0.11
Radiation	CuKα (λ = 1.54184 Å)	MoKα (λ = 0.71073 Å)
2Θ range for data collection/°	5.558 to 153.618	3.49 to 50.246
Index ranges	$-14 \le h \le 14$, $-16 \le k \le 16$, $-20 \le l \le 16$	$-14 \le h \le 15$, $-27 \le k \le 24$, $-15 \le l \le 20$
Reflections collected	51 296	33 438
Independent reflections	10 402 [R_{int} = 0.0300, R_{sigma} = 0.0241]	8265 [R_{int} = 0.0295, R_{sigma} = 0.0266]
Data/restraints/parameters	10 402/227/790	8265/0/599
Goodness-of-fit on F^2	1.026	1.057
Final R indexes [$I \ge 2\sigma(I)$]	R_1 = 0.0399, wR_2 = 0.1071	R_1 = 0.0318, wR_2 = 0.0703
Final R indexes [all data]	R_1 = 0.0467, wR_2 = 0.1130	R_1 = 0.0410, wR_2 = 0.0748
Largest diff. peak/hole/e Å^{-3}	0.84/−0.41	0.27/−0.33

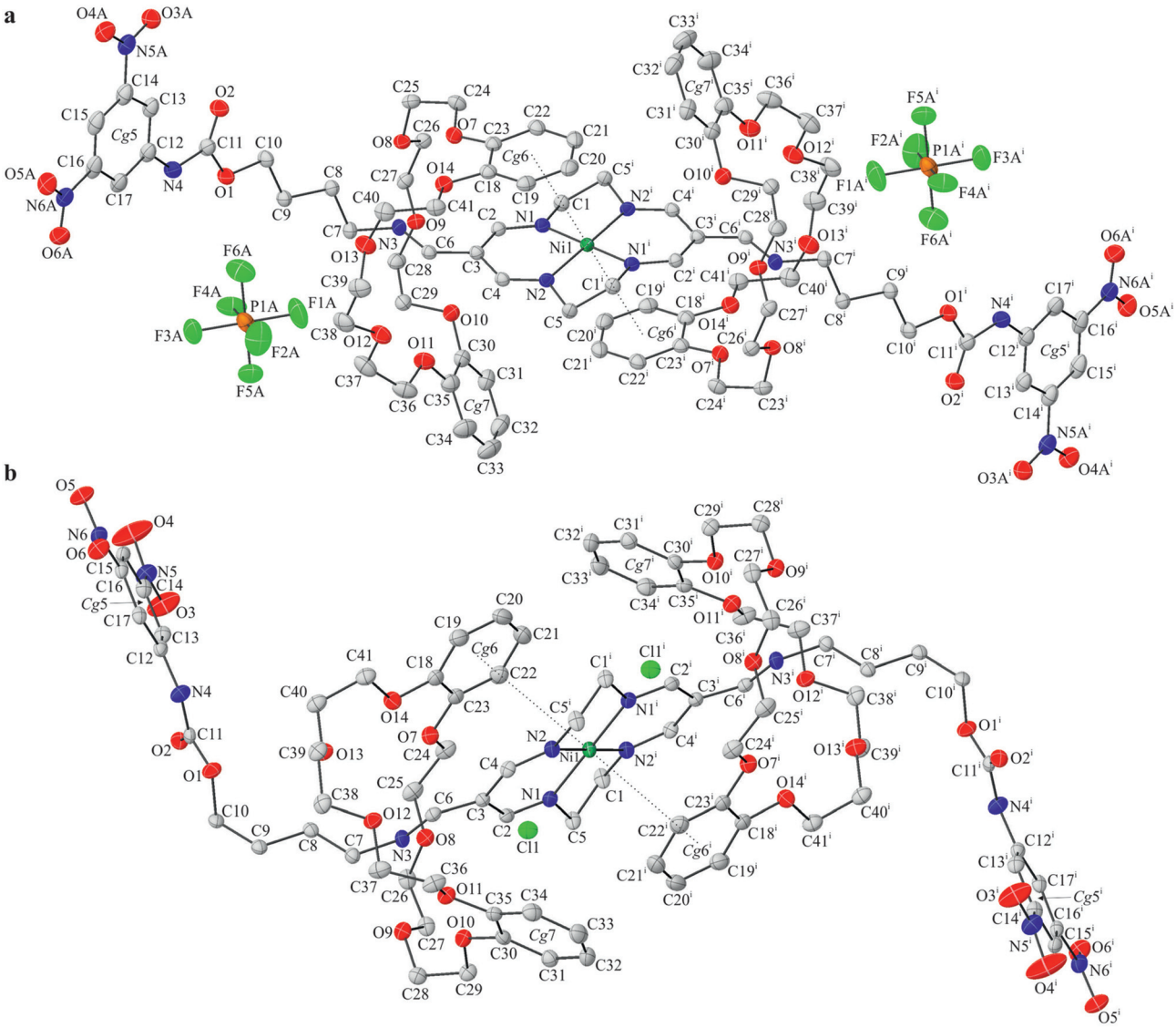

Fig. 2 Molecular structure of **6n** (a) and **6nCl** (b) with atomic labelling scheme. The Ni···π interactions are represented by dotted lines. Hydrogen atoms and molecules of solvents were omitted for clarity. In the case of **6n** only the main parts of disordered fragments are shown. The Cg5, Cg6 and Cg7 denote the geometric centers of gravity of the aromatic rings delineated by the C12–C17, C18–C23 and C30–C35 atoms, respectively. Symmetry code (i): $-x, -y + 2, -z$ (a); $-x + 1, -y + 1, -z + 1$ (b).

Table 2 Selected distances [Å] for **6n** and **6nCl**. The Cg5, Cg6 and Cg7 denote the geometric centers of gravity of the aromatic rings delineated by the C12–C17, C18–C23 and C30–C35 atoms, respectively (Fig. 2 and 17S (ESI)). Symmetry code (i): $-x, -y + 2, -z$ (**6n**); $-x + 1, -y + 1, -z + 1$ (**6nCl**)

	Distance	
A···B	**6n**	**6nCl**
Ni1···Cg6	3.64(2)	3.86(2)
Ni1···Cg7	6.34(2)	5.75(2)
Cg5···Cg5	30.61(2)	25.06(2)
Cg6···Cg7^{i}	5.37(2)	8.22(2)
N3···N3^{i}	11.07(2)	11.03(2)
N4···N4^{i}	25.95(2)	21.93(2)

(Table 10S‡ and Fig. 5). These weak intermolecular interactions play the role of a "glue" which is strengthening the whole crystal structure.

The supramolecular architecture of **6nCl** is presented in Fig. 6. In the crystal of this compound, the neighboring cations and anions are held together by the N–H···Cl and C–H···Cl hydrogen bonds (Fig. 6 and Table 11S‡) involving the fragments of the [3]rotaxane axle and the ether moiety. The molecules of acetonitrile are participating in the weak C–H···N intermolecular interactions with DB24C8 ether wheels (Table 11S‡). The whole crystal structure is stabilized by the network of weak C–H···O hydrogen bonds (Table 11S‡) and C═O···π contacts (Fig. 6b and Table 13S‡) between adjacent [3]rotaxane cations.

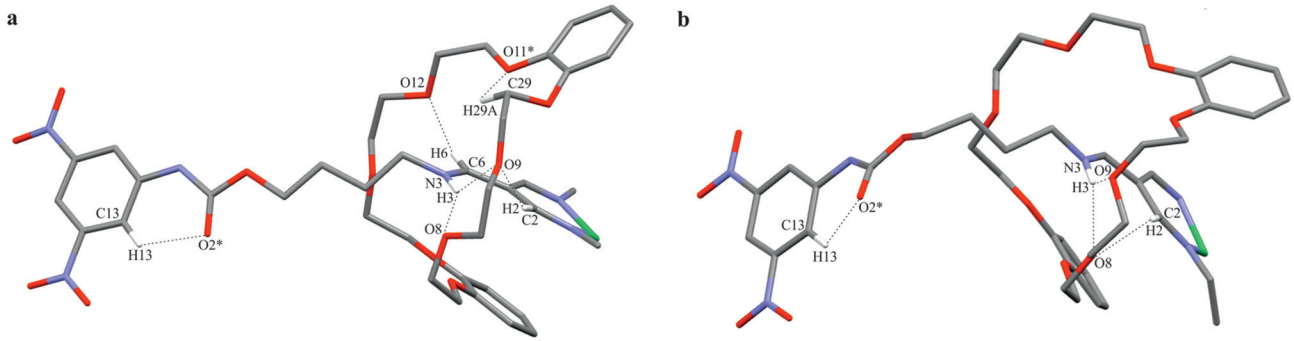

Fig. 3 Illustration of the hydrogen bonds involving fragments of the TAM complex and DB24C8 unit in the independent part of the crystal lattices of **6n** (a) and **6nCl** (b). The N–H···O and C–H···O intermolecular interactions are represented by dashed lines. The H-atoms not involved in these interactions and molecules of solvents were omitted for clarity. Only the main parts of disordered nitro groups are shown. (*) indicates intramolecular interaction.

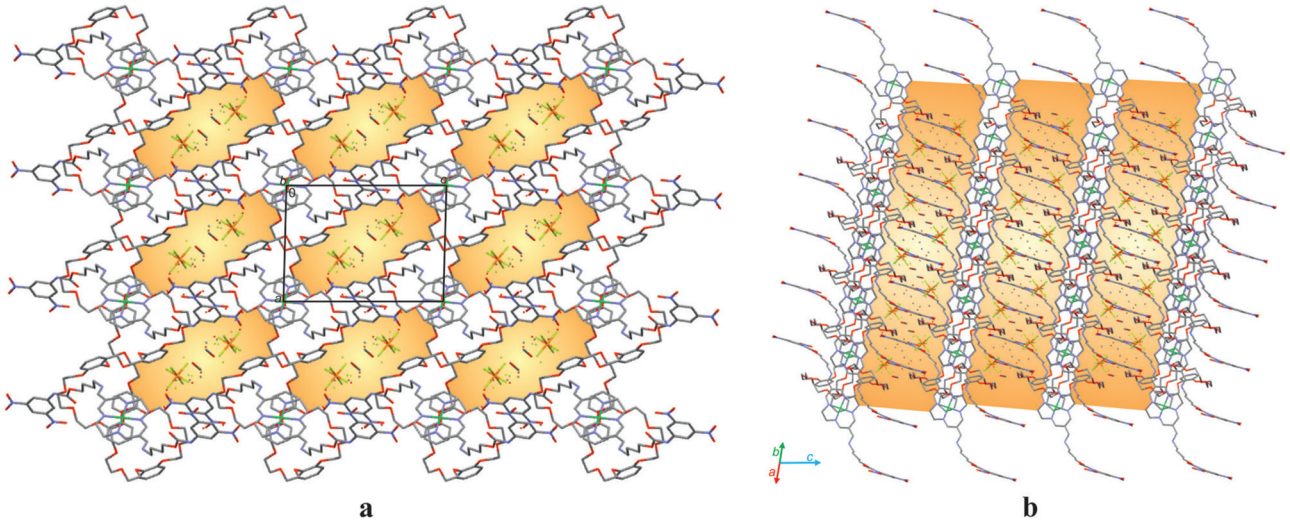

Fig. 4 General view on the packing of moieties in the crystal of **6n**, where (a) projection along the *b*-direction, (b) view from the side. The cavities filled by disordered anions and solvent molecules are highlighted in orange. The H-atoms were omitted for clarity.

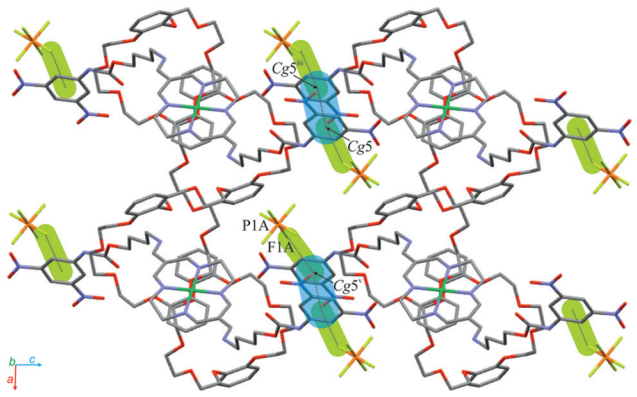

Fig. 5 Illustration of the network of weak intermolecular C–F···π and π–π interactions in the crystal of **6n**. The H-atoms and molecules of solvents were omitted for clarity. Only the main parts of the disordered fragment are shown. The contacts are represented by dotted lines. The C–F···π contacts are highlighted in green, and π–π in blue. Symmetry codes: (iii) $-x, -y, -z+1$, (v) $-x+1, -y, -z+1$.

Electrochemical studies

In the axle molecule **4n**, the nickel(II) ion coordinated by the TAM ligand is electroactive and undergoes one-electron, reversible oxidation to the +3 oxidation state at E_p = 1.11 V (*vs.* non-aqueous Ag/AgCl, Fig. 7). This value of E_p is surprising, since similar nickel(II) TAM complexes have been consistently reported to oxidize at about 1.3 V.[11,12,14–16] This significant difference can be explained by the unprecedented presence of partially negatively charged nitro groups within the **4n** molecule. Nitro groups apparently interact with the positively charged $TAM^{3+/2+}$ unit, stabilizing the higher oxidation state of **4n** and thus lowering the value of its oxidation potential. Dinitroaryl stoppers are also electroactive and their reduction signals are observed at *ca.* −0.7 V.

Upon threading of DB24C8 wheels which encircle the complex moiety, this stabilizing intramolecular interaction becomes impeded. Moreover, excessive steric hindrance, especially in the case of **6n** where the TAM unit is encircled by

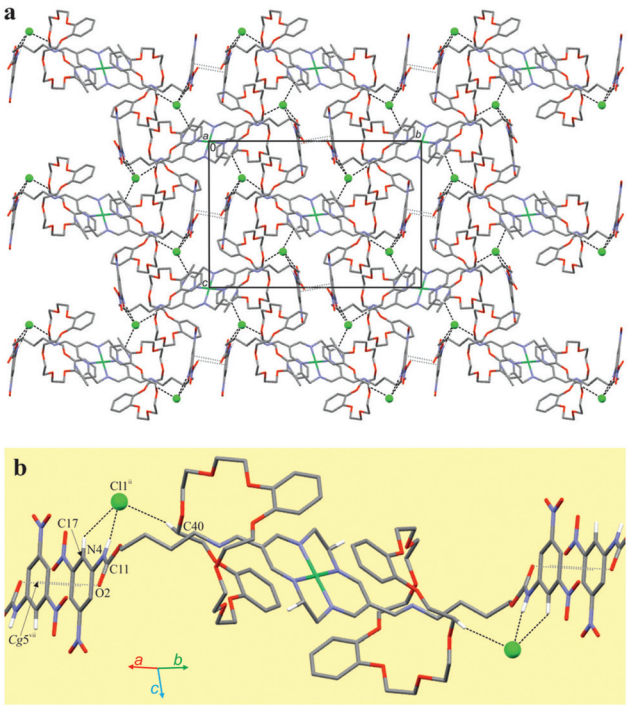

Fig. 6 General view on the packing of ions and solvent molecules in the crystal of **6nCl**, where (a) projection along the *a*-direction and (b) detailed view on the intermolecular interactions in the crystal network. The H-atoms not participating in the interactions between cations and anions were omitted for clarity. The N–H···Cl and C–H···Cl hydrogen bonds are represented by dotted lines and the C=O···π by dotted lines. Symmetry codes: (ii) *x* + 1/2, –*y* + 1/2, *z* – 1/2; (vii) –*x* + 2, –*y*, –*z* + 1.

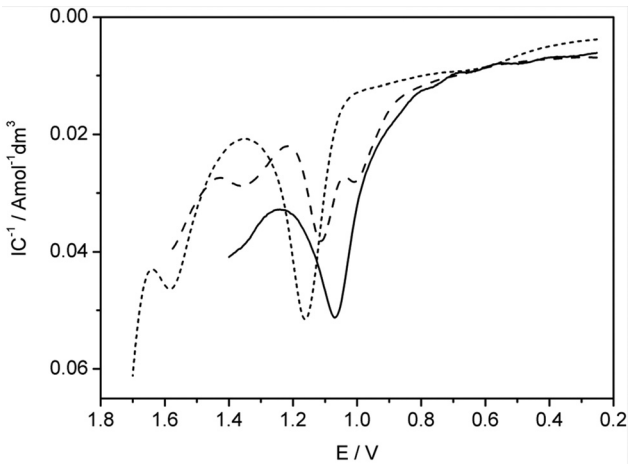

Fig. 7 Differential pulse voltammograms recorded on the GCE in 0.1 M TBAHFP/DMF solution of **4n** – solid line, **5n** – dashed line, **6n** – short-dashed line, amplitude = 50 mV, t_p = 10 ms, reference electrode: Ag/AgCl in methanol.

four catechol rings, results in difficult access of counterions compensating the charge after the oxidation process. Therefore, [2]rotaxane **5n** and [3]rotaxane **6n** oxidize at slightly higher potentials than the axle: 1.14 and 1.18 V, respectively

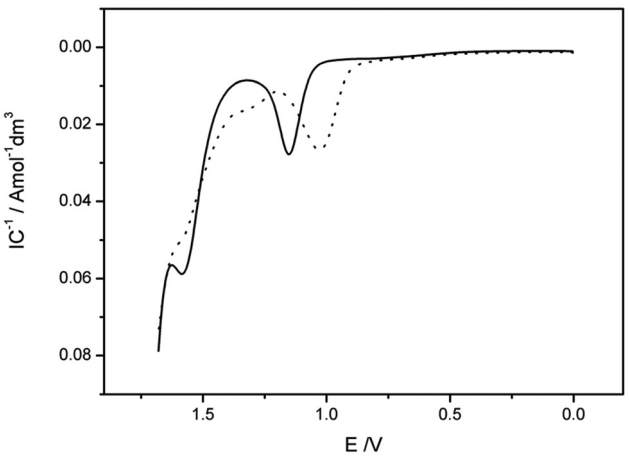

Fig. 8 Square wave voltammograms recorded on the GCE in 0.1 M TBAHFP/DMF solution of **6n** – solid line, **6nCl** – dotted line, frequency = 5 Hz, reference electrode: Ag/AgCl in methanol.

(Fig. 7). In our previous studies [2]rotaxanes always oxidized easier than the corresponding axles due to the stabilization coming from π–π interaction between DB24C8 and $TAM^{3+/2+}$ units.[11,12,14–16] Here, the order of E_p values is reversed, simply because the stabilizing effect of nitro groups is stronger than that of DB24C8. Irreversible oxidation of DB24C8 is placed at about 1.60 V as reported earlier.[16,17]

In the case of **5n**, the second peak was observed during voltammetric measurements at 1.01 V (Fig. 7). This signal corresponds to the redox process of the +1 charged product of proton dissociation from **5n** (both exocyclic NH proton and protons in carbamate groups are acidic). Indeed, an additional experiment in which triethylamine was added to the solution resulted in the expected enhancement of the 1.01 V signal and disappearance of the 1.14 V one (Fig. 18S (ESI‡)). Similar dissociation-related effects on the electrochemical behavior of the TAM complex were observed in the previous paper.[16] Moreover, this observation is in accordance with ^{1}H NMR data, where acidic protons in **5n** (and only in **5n**) were shown to be labile and participating in chemical exchange.

Upon replacing the hexafluorophosphate counterions in **6n** by chloride ions in **6nCl**, the nickel(II) oxidation potential in [3]rotaxane shifts even more toward less positive values: 1.03 V (Fig. 8). This can be explained similarly to the influence of nitro groups. The coordinating chloride ions, which are additionally smaller than PF_6^- in **6n**, diffuse to the center of the molecule and stabilize the higher oxidation state more easily.

Experimental

Materials and methods

Acetonitrile and dichloromethane were dried over P_2O_5, distilled and stored under Ar. Toluene was dried with sodium, distilled and stored with Na and under Ar. All other solvents and reagents were used without additional purification: 3,5-

dimethoxybenzoyl chloride (>98%, TCI Chemicals,); 3,5-dinitrobenzoyl chloride for fluorescence (>98.0%, Aldrich); sodium azide (POCh); methyl trifluoromethanesulfonate (>98%, Aldrich); 4-amino-1-butanol (>98%, TCI Chemicals); ammonium hexafluorophosphate (99.8%, Apollo Scientific); dibenzo-24-crown-8 (>98%, TCI Chemicals); silica gel 60 H for thin-layer chromatography (Merck); aluminium oxide 60 GF254 neutral (type E) for thin-layer chromatography (Merck); silica gel 60 silanized for column chromatography (0.063–0.200 mm, Merck). 3,5-Dimethoxybenzoyl and 3,5-dinitrobenzoyl azides were stored in a dry and sealed container within a freezer.

Synthetic procedures

Equipment: Elemental analyzer PERKIN-ELMER type 240; mass spectrometer MALDI Synapt G2-S; nuclear magnetic resonance spectrometers Varian VNMRS 600 MHz and Varian Mercury 400 MHz (chemical shifts reported in reference to acetonitrile residual peak (1.94 ppm (^{1}H) and 118.26 ppm (^{13}C)). The assignment of the ^{13}C signals was supported by ^{1}H–^{13}C HSQC spectra.

Complex **1**: This compound was synthesized according to the new, one-pot synthesis.[45]

Complex **2**: Methyl trifluoromethanesulfonate (721.1 μl, 6.372 mmol, 2.1 eq.) was added to the refluxing suspension of **1** (924.6 mg, 3.032 mmol, 1.0 eq.) in CH_2Cl_2 (100 ml, anhyd.). After 4 h of stirring at reflux, 4-aminobutan-1-ol (587.4 μl, 6.372 mmol, 2.1 eq.) was added and the heat source was removed. 15 min later, the suspension was evaporated to dryness. Purification was performed on a silanized silica gel column, with an eluent composed of NH_4PF_6, CH_3CN and H_2O (10 mg : 1.0 ml : 1.5 ml). The first fraction was partially concentrated yielding an orange-coloured precipitate. The title compound was filtered, rinsed with H_2O, dried and stored *in vacuo* over P_2O_5. Yield 1.669 g (74%). Anal. calc. for $C_{20}H_{34}N_6NiO_2{\cdot}2PF_6$ (739.15): C 32.50, H 4.64, N 11.37%; found C 32.24, H 4.87, N 11.27%. TOF MS ES$^+$ (CH_3CN, *m*/*z*): 224.1 $[M]^{2+}$. ^{1}H NMR (400 MHz, CD_3CN) δ 1.51–1.59 (m, 4 H, CH_2CH_2OH); 1.68–1.76 (m, 4 H, CH_2CH_2NH); 2.73 (br s, 2 H, OH); 3.47–3.62 (m, 16 H, $N(CH_2)_2N$, CH_2NH, CH_2OH); 7.49, 7.51, 7.95 and 7.97 (4 × s, 4 × 1 H, CH=N); 7.66 (d, J = 14.8 Hz, 2 H, =CHN); 8.28 (very br s, 2 H, NH). ^{13}C NMR (100 MHz, CD_3CN) δ 27.3, 30.0 ($NHCH_2(CH_2)_2CH_2OH$); 51.6, 61.9 ($NHCH_2(CH_2)_2CH_2OH$); 59.3, 59.5, 60.2 and 60.4 ($N(CH_2)_2N$); 104.1 (C=CHN); 155.0 and 160.6 (CH=N); 163.9 (=CHN).

3,5-Dimethoxybenzoyl azide (**3m**): A solution of 3,5-dimethoxybenzoyl chloride (4.022 g, 0.020 mol, 1 eq.) in acetone (10 ml) was added dropwise over 30 min to the ice-cold solution of NaN_3 (2.610 g, 0.040 mmol, 2 eq.) in H_2O (10 ml). After 1 h of stirring, acetone was evaporated on a rotovap without heating. The precipitate was filtered, rinsed with H_2O, and purified on silicagel with CH_2Cl_2/*n*-hexane ($1 : 1_{vol}$) as an eluent. The first major fraction was evaporated to dryness (without heating) to give the title compound as a colourless solid. Yield: 3.314 g (80%). ^{1}H NMR (400 MHz, $CDCl_3$): 3.84 (s, 6 H, CH_3), 6.69 (t, J = 2.4 Hz, 1 H, H_{Ar} *para* to CON_3), 7.17 (d, J = 2.4 Hz, 2 H, H_{Ar} *ortho* to CON_3). ^{13}C NMR (100 MHz, $CDCl_3$): 55.8 (CH_3), 107.1 (C_{sp^2}–H "*ortho*" to CON_3), 107.3 (C_{sp^2}–H "*para*" to CON_3), 132.6 (C_{sp^2}–CON_3), 161.0 (C_{sp^2}–O), 172.4 (CON_3).

3,5-Dinitrobenzoyl azide (**3n**) was synthesized from 3,5-dinitrobenzoyl chloride according to the above described procedure. Caution should be exercised as the compound may explode at elevated temperature. Yield: 91%. ^{1}H NMR (400 MHz, $CDCl_3$): 9.15 (d, J = 2.1 Hz, 2 H, H_{Ar} *ortho* to CON_3), 9.25 (t, J = 2.1 Hz, 1 H, H_{Ar} *para* to CON_3). ^{13}C NMR (100 MHz, $CDCl_3$): 123.4 (C_{sp^2}–H "*para*" to CON_3), 129.2 (C_{sp^2}–H "*ortho*" to CON_3), 134.2 (C_{sp^2}–CON_3), 149.0 (C_{sp^2}–NO_2), 168.9 (CON_3).

4m: 3,5-Dimethoxybenzoyl azide (114.4 mg, 0.55 mmol, 3 eq.) was closed under an argon atmosphere in a dry, two-neck flask equipped with a balloon. The flask was immersed in an oil bath preheated to 100 °C. After 3 h of heating and stirring, the product was allowed to cool to RT and 1 ml of a solution of **2** (135.3 mg, 0.183 mmol, 1 eq.) in anhyd. CH_3CN was added through a silicone stopper. The solution was allowed to stand at RT for 12 h, followed by evaporation to dryness. The resulting orange-coloured solid was purified on a silanized silica gel column, with an eluent composed of NH_4PF_6, CH_3CN and H_2O (10 mg : 1 ml : 1 ml). The last/major fraction was partially concentrated yielding an orange-coloured precipitate. The title compound was filtered, rinsed with H_2O, dried and stored *in vacuo* over P_2O_5. Yield 144.1 mg (71%). Anal. calc. for $C_{38}H_{52}N_8NiO_8{\cdot}2PF_6{\cdot}H_2O$ (1115.51): C 40.92, H 4.88, N 10.04%; found C 40.93, H 4.87, N 10.01%. TOF MS ES$^+$ (CH_3CN, *m*/*z*): 403.2 $[M]^{2+}$. ^{1}H NMR (600 MHz, CD_3CN) δ 1.69–1.80 (comp, 8 H, $CH_2(CH_2)_2CH_2$); 3.38–3.58 (br m, 8 H, $N(CH_2)_2N$); 3.54 (t, J = 6.4 Hz, 4 H, $NHCH_2$); 3.73 (s, 12 H, CH_3); 4.15 (t, J = 6.1 Hz, 4 H, CH_2OCO); 6.19 (t, J = 2.2 Hz, 2 H, H_{Ar} *para* to $NHCO_2$); 6.65 (d, J = 2.0 Hz, 4 H, H_{Ar} *ortho* to $NHCO_2$); 7.66 (br s, 2 H, =CHN); 7.3–8.4 (set of broad signals, 8 H, CH=N, NH). ^{13}C NMR (150 MHz, CD_3CN) δ 26.4 and 26.8 ($CH_2(CH_2)_2CH_2$), 51.1 ($NHCH_2$), 55.9 (CH_3), 59.0–60.5 br ($N(CH_2)_2N$), 64.9 (CH_2OCO), 95.6 (C_{sp^2}–H "*para*" to $NHCO_2$), 97.8 (C_{sp^2}–H "*ortho*" to $NHCO_2$), 104.3 (C=CHN), 141.6 (C_{sp^2}–$NHCO_2$), 154.5 (C=O), 155.0 br and 160.6 br (CH=N), 162.2 (C_{sp^2}–OMe), 164.0 (=CHN).

4n: Neat 3,5-dinitrobenzoyl azide explodes at elevated temperatures and needs to be rearranged in the presence of a solvent. A solution of 3,5-dinitrobenzoyl azide (105.0 mg, 0.443 mmol, 2.5 eq.) in anhyd. toluene (1.1 ml) was closed under an argon atmosphere in a dry, two-neck flask equipped with a condenser and balloon. The flask was immersed in an oil bath preheated to 120 °C. After 3 h of heating and stirring, the solution was allowed to cool to RT. 2 ml of a solution of **2** (130.8 mg, 0.177 mmol, 1 eq.) in anhyd. CH_3CN was then added through a silicone stopper. The mixture was stirred overnight at RT and then evaporated to dryness. CH_3CN was added to the yellow solid thus obtained, and the suspension was sonicated in an ultrasonic bath for 15 min, followed by stirring at reflux for 15 min. Filtration yielded an orange filtrate (discarded) and some insoluble material which was washed with CH_3CN and *n*-hexane. After drying *in vacuo* over P_2O_5 the

poorly soluble solid was confirmed to be the title compound in its pure form. Yield 88.2 mg (43%). Anal. calc. for $C_{34}H_{40}N_{12}NiO_{12}\cdot 2PF_6$ (1157.38): C 35.28, H 3.48, N 14.52%; found C 35.30, H 3.54, N 14.54%. TOF MS ES$^+$ (CH_3CN, *m*/*z*): 433.3 $[C_{34}H_{40}N_{12}NiO_{12}]^{2+}$. ^{1}H NMR (600 MHz, CD_3CN) δ 1.72–1.80 (comp, 8 H, $CH_2(CH_2)_2CH_2$); 3.44–3.60 (comp, 12 H, $N(CH_2)_2N$ and $NHCH_2$); 4.22 (br m, 4 H, CH_2OCO); 7.584, 7.593 and 8.289, 8.298 (4 × s, 4 × 1 H, CH═N); 7.88 (d, *J* = 15.6 Hz, 2 H, ═CHN); 8.50 (t, *J* = 2.1 Hz, 2 H, H_{Ar} *para* to $NHCO_2$); 8.68 (d, *J* = 1.8 Hz, 4 H, H_{Ar} *ortho* to $NHCO_2$); 9.92–10.0 (m, 2 H, $NHCH_2$); 10.13 (br s, 2 H, $NHCO_2$). ^{13}C NMR (150 MHz, CD_3CN) δ 26.4 and 26.9 ($CH_2(CH_2)_2CH_2$), 51.3 ($NHCH_2CH_2$), 59.2, 59.4, 60.1, 60.4 ($N(CH_2)_2N$), 65.7 (CH_2OCO), 104.5 (C═CHN), 112.5 (C_{sp^2}–H "*para*" to $NHCO_2$), 118.6 (C_{sp^2}–H "*ortho*" to $NHCO_2$), 143.0 (C_{sp^2}–$NHCO_2$), 149.8 (C_{sp^2}–NO_2), 154.7 (C═O), 155.7 and 160.7 (CH═N), 164.6 (═CHN).

Rotaxanes **5m** and **6m**: 3,5-Dimethoxyphenyl isocyanate was prepared from 3,5-dimethoxybenzoyl azide (350.3 mg, 1.691 mmol, 2.5 eq.) as in the procedure for **4m**. After cooling to RT, CH_2Cl_2 (5 ml) was added through a silicone stopper and the syringe was filled with the resulting solution. The emptied flask was loaded with a solution of DB24C8 (3.031 g, 6.758 mmol, 10 eq.) in CH_2Cl_2 (9 ml). Isocyanate/CH_2Cl_2 and a solution of **2** (499.7 mg, 0.676 mmol, 1 eq.) in CH_3CN (5 ml, second syringe) were simultaneously added dropwise to DB24C8/CH_2Cl_2 over 3 h. The mixture was stirred overnight, evaporated to dryness, redissolved in CH_2Cl_2, and poured onto an alumina DCVC column (40 g). An excess of DB24C8 was separated during elution with CH_2Cl_2. Then, an orange-colored band of cationic complexes was forced to leave the column with a NH_4PF_6/CH_3CN (10 g l^{-1}) solution. The resulting mixture was evaporated to dryness and applied to a silanized silica gel column. RP chromatographic separation was performed by means of gradient elution with 40–70%$_{vol.}$ of NH_4PF_6/CH_3CN (10 g l^{-1}) in H_2O. Minor bands were discarded, whereas two major orange-coloured fractions were partially concentrated yielding oily precipitates. Samples were filtered, rinsed with H_2O, dissolved in CH_2Cl_2, separated from an excess of water, precipitated with *n*-hexane, and dried and stored *in vacuo* over P_2O_5. Yields: 253.9 mg (24%) of **5m** and 170.5 mg (13%) of **6m**. For [2]rotaxane **5m**: anal. calc. for $C_{62}H_{84}N_8NiO_{16}\cdot 2PF_6$ (1546.00): C 48.17, H 5.48, N 7.25%; found C 48.20, H 5.58, N 7.10%. TOF MS ES$^+$ (CH_3CN, *m*/*z*): 627.5 $[M]^{2+}$. ^{1}H NMR (600 MHz, CD_3CN) δ 1.69–1.79 and 1.80–89 (2 × m, 2 × 4 H, $CH_2(CH_2)_2CH_2$); 2.85–2.96 (2 H), 3.11–3.17 (1 H), 3.18–3.28 (3 H), 3.29–3.34 (1 H), and 3.37–3.41 (1 H) (5 × m, Σ 8 H, $N(CH_2)_2N$); 3.52 (t, *J* = 6.4 Hz, 2 H, $NHCH_2$); 3.64–3.69 (m, 2 H, $NHCH_2$); 3.69–3.77 (comp, all 8 of $CH_2O(CH_2)_2O$ and 4 of $ArOCH_2CH_2$); 3.70 (s, 6 H, CH_3 (crown side)); 3.74 (s, 6 H, CH_3 (bare side)); 3.79–3.83 (m, 4 of $ArOCH_2$); 3.95–4.01 (m, 4 of $ArOCH_2CH_2$); 4.05–4.10 (m, 4 of $ArOCH_2$); 4.16 (t, *J* = 6.2 Hz, 2 H, CH_2OC═O); 4.21–4.25 (br t, 2 H, CH_2OC═O); 6.16 and 6.20 (2 × t, *J* = 2.2 Hz, 2 × 1 H, H_{Ar} *para* to $NHCO_2$); 6.63 and 6.68 (2 × d, *J* = 2.0 Hz, 2 × 2 H, H_{Ar} *ortho* to $NHCO_2$); 6.63 and 7.59 (2 × s, 2 × 1 H, CH═N, overlayed with a doublet at 6.63 ppm, and respectively, doublet at 7.59 ppm); 6.77–6.83 (m, 8 H, H_{Ar} of the crown ether); 7.31, 7.37, 7.85 and 7.91 (4 × s, 4 × 0.5 H, CH═N); 7.59 and 8.18 (2 × d, *J* = 15.1 and 16.0 Hz, 2 × 1 H, ═CHN); 7.66 and 7.73 (2 × br s, 2 × 1 H, $NHCO_2$); 8.10 (very br, 1 H, $NHCH_2$ (bare side)); 8.72–8.81 (m, 1 H, $NHCH_2$ (crown side)). ^{13}C NMR (150 MHz, CD_3CN) δ 26.4, 26.9, 27.1 and 27.3 ($CH_2(CH_2)_2CH_2$); 51.0 and 51.1 ($NHCH_2$); 55.85 and 55.92 (CH_3); 58.48, 59.67, 59.09, 59.11, 59.42, 59.62, 59.98 and 60.01 ($N(CH_2)_2N$); 64.9 and 65.2 (CH_2OCO); 68.3 ($ArOCH_2$); 71.0 ($ArOCH_2CH_2$); 71.3 ($CH_2O(CH_2)_2O$); 95.68 and 95.73 (C_{sp^2}–H "*para*" to $NHCO_2$); 97.66 br and 97.78 br (C_{sp^2}–H "*ortho*" to $NHCO_2$); 104.2 and 104.4 (C═CHN); 112.8 (C_{sp^2}–H "*ortho*" to OCH_2); 121.7 (C_{sp^2}–H "*meta*" to OCH_2); 141.6 (C_{sp^2}–$NHCO_2$); 148.9 (C_{sp^2}–OCH_2); 154.6 (C═O); 154.65, 154.77, 158.77, 158.80, 160.03 and 160.19 (CH═N); 162.1 and 162.2 (C_{sp^2}–OMe); 163.5 (═CHN (bare side)); 166.9 (═CHN (crown side)). For [3]rotaxane **6m**: anal. calc. for $C_{86}H_{116}N_8NiO_{24}\cdot 2PF_6$ (1994.51): C 51.79, H 5.86, N 5.62%; found C 51.60, H 5.69, N 5.67%. TOF MS ES$^+$ (CH_3CN, *m*/*z*): 851.6 $[M]^{2+}$. ^{1}H NMR (600 MHz, CD_3CN) δ 1.71 (br comp, 8 H, $CH_2(CH_2)_2CH_2$); 2.67 and 3.03 (2 × br s, 2 × 2 H, $N(CH_2)_2N$); 2.82 and 2.95 (2 × br t, *J* = 6.4 and 6.3 Hz, 2 × 2 H, $N(CH_2)_2N$); 3.52–3.60 (br m, 4 H, $NHCH_2$); 3.65–3.77 (br m, 16 H, $CH_2O(CH_2)_2O$); 3.71 (s, 12 H, CH_3); 3.70–3.76 and 3.88–3.94 (2 × br m, 2 × 8 H, $ArOCH_2CH_2$); 3.95–4.01 and 4.04–4.10 (2 × br m, 2 × 8 H, $ArOCH_2$); 4.09–4.15 (br m, 4 H, CH_2OCO); 6.17 (t, *J* = 2.2 Hz, 2 H, C_{sp^2}–H *para* to $NHCO_2$); 6.64 (d, *J* = 2.1 Hz, 4 H, C_{sp^2}–H *ortho* to $NHCO_2$); 6.69 and 6.78 (2 × br s, 2 × 1 H, CH═N); 6.81–6.88 (m, 16 H, H_{Ar} in the crown ether); 7.61–7.65 (comp, 4 H, CH═N and $NHCO_2$); 8.10 (d, *J* = 15.9 Hz, 2 H, ═CHN); 8.56–8.65 (m, 2 H, $NHCH_2$). ^{13}C NMR (150 MHz, CD_3CN) δ 27.0 and 27.1 ($CH_2(CH_2)_2CH_2$); 51.0 ($NHCH_2$); 55.9 (CH_3); 58.7, 59.6, 59.7 ($N(CH_2)_2N$); 65.1 (CH_2OCO); 68.6 ($ArOCH_2$); 71.0 ($ArOCH_2CH_2$); 71.5 ($CH_2O(CH_2)_2O$); 95.7 (C_{sp^2}–H "*para*" to $NHCO_2$); 97.7 (C_{sp^2}–H "*ortho*" to $NHCO_2$); 104.06 and 104.11 (C═CHN); 113.0 (C_{sp^2}–H "*ortho*" to OCH_2); 121.9 (C_{sp^2}–H "*meta*" to OCH_2); 141.6 (C_{sp^2}–$NHCO_2$); 148.9 (C_{sp^2}–OCH_2); 154.5 (C═O); 154.8, 154.9, 158.9 and 159.2 (CH═N); 162.1 (C_{sp^2}–OMe); 166.5 (═CHN).

Rotaxanes **5n** and **6n**: 3,5-Dinitrophenyl isocyanate was prepared from 3,5-dinitrobenzoyl azide (417.8 mg, 1.762 mmol, 2.5 eq.) as in the procedure for **4n**. Rotaxanes were synthesized and purified following the above described procedure for their methoxy-congeners. Two major orange-coloured fractions collected from the column yielded crystalline precipitates which were filtered, rinsed with H_2O, *n*-hexane and dried and stored *in vacuo* over P_2O_5. Yields: 320.1 mg (28%) of **5n** and 232.6 mg (16%) of **6n**. For [2]rotaxane **5n**: anal. calc. for $C_{58}H_{72}N_{12}NiO_{20}\cdot 2PF_6$ (1605.88): C 43.38, H 4.52, N 10.47%; found C 43.17, H 4.57, N 10.47%. TOF MS ES$^+$ (CH_3CN, *m*/*z*): 657.4 $[M]^{2+}$. ^{1}H NMR (600 MHz, CD_3CN) δ 1.75–1.79 (br comp, 4 H, $CH_2(CH_2)_2CH_2$ (bare side)); 1.82–1.92 (br comp, 4 H, $CH_2(CH_2)_2CH_2$ (crown side)); 2.89 and 3.22 (2 × br t, *J* = 6.6 Hz, 2 × 2 H, $N(CH_2)_2N$); 3.16 and 3.34 (2 × br s, 2 × 2 H, $N(CH_2)_2N$); 3.50–3.56 and 3.64–3.69 (2 × br m, 2 × 2 H, $NHCH_2$); 3.69–3.74 (m, 4 H, $ArOCH_2CH_2$); 3.77 (s, 8 H, $CH_2O(CH_2)_2O$); 3.78–3.82 (m, 4 H, $ArOCH_2$); 3.98–4.08 (comp, 8 H, 4 of $ArOCH_2$ and 4 of

$ArOCH_2C\underline{H}_2$); 4.24–4.28 (m, 2 H, CH_2OCO (bare side)); 4.35 (t, J = 6.0 Hz, 2 H, CH_2OCO (crown side)); 6.63 and 7.59 (2 × s, 2 × 1 H, CH═N (crown side)); 6.72–6.78 (br m, 8 H, H_{Ar} in the crown ether); 7.36 and 7.82 (2 × br s, 2 × 1 H, CH═N (bare side)); 7.58 (s, 1 H, ═CHN (bare side)); 7.97 (br s, 1 H, $N\underline{H}CH_2$ (bare side)); 8.18 (d, J = 16.2 Hz, 1 H, ═CHN (crown side)); 8.40 (s, 1 H, $NHCO_2$ (crown side)); 8.41 (t, J = 2.0 Hz, 1 H, C_{sp^2}–H *para* to $NHCO_2$ (crown side)); 8.45 (br s, 1 H, $NHCO_2$ (bare side)); 8.55 (t, J = 2.0 Hz, 2 H, C_{sp^2}–H *ortho* to $NHCO_2$ (crown side)); 8.57 (d, J = 2.0 Hz, 1 H, C_{sp^2}–H *para* to $NHCO_2$ (bare side)); 8.68 (d, J = 1.9 Hz, 2 H, C_{sp^2}–H *ortho* to $NHCO_2$ (bare side)); 8.75–8.83 (m, 1 H, $N\underline{H}CH_2$ (crown side)). ^{13}C NMR (150 MHz, CD_3CN) δ 26.3, 26.9, 27.3 and 27.4 ($CH_2(\underline{C}H_2)_2CH_2$); 51.0 and 51.1 ($NH\underline{C}H_2$); 58.6 br and 59.5 br ($N(CH_2)_2N$); 66.0 and 66.3 ($\underline{C}H_2OCO$); 68.3 ($ArOCH_2$); 71.0 ($ArOCH_2\underline{C}H_2$); 71.3 ($CH_2O(\underline{C}H_2)_2O$); 104.2 and 104.4 ($\underline{C}$═CHN); 112.7 ($C_{sp^2}$–H "*ortho*" to OCH_2); 112.8 and 113.0 (C_{sp^2}–H "*para*" to $NHCO_2$); 118.8 (C_{sp^2}–H "*ortho*" to $NHCO_2$, the second one overlayed with a solvent residual signal); 121.7 (C_{sp^2}–H "*meta*" to OCH_2); 142.3 and 142.4 (C_{sp^2}–$NHCO_2$); 148.9 ($\underline{C}_{sp^2}$–OCH_2); 149.6 and 149.8 (C_{sp^2}–NO_2); 154.4 and 154.5 (C═O); 154.8 and 158.9 (CH═N); 163.5 and 167.0 (═CHN). For [3]rotaxane **6n**: anal. calc. for $C_{82}H_{104}N_{12}NiO_{28}\cdot 2PF_6$ (2054.39): C 47.94, H 5.10, N 8.18%; found C 47.90, H 5.24, N 7.97%. TOF MS ES$^+$ (CH_3CN, m/z): 881.5 $[M]^{2+}$. ^{1}H NMR (600 MHz, CD_3CN) δ 1.77 (br comp, 8 H, $CH_2(C\underline{H}_2)_2CH_2$); 2.56 and 2.95 (2 × br s, 2 × 2 H, $N(CH_2)_2N$); 2.72 and 2.86 (2 × br t, J = 6.4 and 6.4 Hz, 2 × 2 H, $N(CH_2)_2N$); 3.54–3.62 (br m, 4 H, $NHC\underline{H}_2$); 3.66–3.78 (comp, 24 H, 8 of $ArOCH_2C\underline{H}_2$ and 16 of $CH_2O(C\underline{H}_2)_2O$); 3.91–3.98 (comp, 16 H, 8 of $ArOCH_2$ and 8 of $ArOCH_2C\underline{H}_2$); 4.01–4.08 (br m, 8 H, $ArOCH_2$); 4.23–4.29 (br m, 4 H, CH_2OCO); 6.61 and 6.72 (2 × br s, 2 × 1 H, CH═N); 6.75–6.80 (br m, 16 H, H_{Ar} of the crown ether); 7.56 and 7.57 (2 × s, 2 × 1 H, CH═N); 8.08 (d, J = 15.8 Hz, 2 H, ═CHN); 8.37 (s, 2 H, $NHCO_2$); 8.42 (br s, 2 H, C_{sp^2}–H *para* to $NHCO_2$); 8.56 (br s, 4 H, C_{sp^2}–H *ortho* to $NHCO_2$); 8.60–8.67 (m, 2 H, $N\underline{H}CH_2$). ^{13}C NMR (150 MHz, CD_3CN) δ 27.12, 27.17, 27.27 and 27.32 ($CH_2(\underline{C}H_2)_2CH_2$); 50.9 ($NH\underline{C}H_2$); 58.60, 59.59 and 59.62 ($N(CH_2)_2N$); 66.2 ($\underline{C}H_2OCO$); 68.52 and 68.55 ($ArOCH_2$); 71.0 ($ArOCH_2\underline{C}H_2$); 71.5 ($CH_2O(\underline{C}H_2)_2O$); 104.0 and 104.1 ($\underline{C}$═CHN); 112.8 ($C_{sp^2}$–H "*para*" to $NHCO_2$); 112.9 (C_{sp^2}–H "*ortho*" to OCH_2); ~118 (C_{sp^2}–H "*ortho*" to $NHCO_2$, overlayed with a solvent residual signal); 121.8 (C_{sp^2}–H "*meta*" to OCH_2); 142.3 (C_{sp^2}–$NHCO_2$); 148.8 ($\underline{C}_{sp^2}$–OCH_2); 149.6 (C_{sp^2}–NO_2); 154.4 (C═O); 154.7, 154.8, 158.8 and 159.1 (CH═N); 166.6 (═CHN).

6nCl: Bis(hexafluorophosphate) [3]rotaxane **6n** (78.5 mg, 0.038 mmol) was dissolved in CH_3CN (1.5 ml) and a solution of tetrabutylammonium chloride (21.2 mg, 2 eq.) in CH_3CN (1 ml) was added. **6nCl** precipitated instantaneously, was filtered, rinsed with CH_3CN and recrystallized from acetone/methanol. These crystals were subjected to X-ray crystallographic studies. Anal. calc. for $C_{82}H_{104}N_{12}NiO_{28}\cdot 2Cl$ (1835.37): C 53.66, H 5.71, N 9.16%; found C 53.59, H 5.80, N 9.11%.

X-ray crystallographic studies

Good quality single-crystal specimens of **6n** and **6nCl** were selected for X-ray diffraction data collection. Diffraction data were collected at 100(2) K on the Agilent Technologies SuperNova Dual (**6n**) or Single Source (**6nCl**) diffractometers with CuKα (λ = 1.54184 Å) (**6n**) and MoKα (λ = 0.71073 Å) (**6nCl**) using CrysAlis RED software.[46] The crystals were positioned at ~70 mm from the ATLAS CCD detector and at ~50 mm from the EOS CCD detector, respectively. A complete data set was collected at 1° intervals with counting time ranges 2.5–15 and 10–70 s for **6n** and **6nCl**, respectively. In total, 5294 and 669 frames were collected for **6n** and **6nCl**, respectively. The analytical numerical absorption correction using a multifaceted crystal model based on expressions derived by R. C. Clark & J. S. Reid[47] (**6nCl**) and numerical absorption correction based on Gaussian integration over a multifaceted crystal model (**6n**) implemented in SCALE3 ABSPACK scaling algorithm, were applied.[46] The data were corrected for Lorentzian and polarization effects. Data reduction and analysis were carried out with the CrysAlis program.[46] The structure determination procedure was carried out using the SHELX package.[48] The structure was solved by direct methods and then successive least-squares refinement was carried out based on the full-matrix least-squares method on F^2 using the SHELXL program. The hydrogen atoms, except those linked to the O-atom of the water molecule in **6n**, and imine N-atoms in **6nCl**, were positioned geometrically, with X–H equal to 0.84, 0.88, 0.95 and 0.99 Å for hydroxyl, imine, aromatic, methyl and methylene H-atoms, respectively in **6n**, and 0.85, 0.93, 0.96 and 0.97 for imine, aromatic, methylene and methyl H-atoms, respectively in **6nCl**, and constrained to ride on their parent atoms with $U_{iso}(H) = xU_{eq}(C,N,O)$, where x = 1.2 for the aromatic, methylene and imine H-atoms, and x = 1.5 for the methyl and hydroxyl H-atoms. The H-atoms of the water molecule in **6n** and those linked to the imine N-atoms in **6nCl** were located on a Fourier difference map and constrained to ride on their parent atom with $U_{iso}(H) = xU_{eq}(O,N)$, where x = 1.2 or 1.5 for N or O-atom, respectively. All nitro groups of the [3]rotaxaneaxle, and the PF_6^- anions in **6n** are disordered in two positions with the site occupancy factors of 0.59 : 0.41 and 0.89 : 0.11 for the nitro groups and the PF_6^- counterions, respectively. Occupancy parameters of solvent moieties in **6nCl** were less than 100% and they were refined freely; thus solvent molecules were in a non-stoichiometric ratio to the main [3]rotaxane moiety. The atoms of disordered parts of the structures were subject to numerous SADI, DELU and RIGU restraints.

The figures for this publication were prepared using Olex2 and Mercury programs.[49] All molecular interactions in the crystal were identified using the PLATON program.[50]

CCDC 1856147 and 1856148‡ contain the supplementary crystallographic data.

Electrochemical studies

Electrochemical experiments were carried out using a CH Instrument 650D potentiostat (CH Instruments, Inc., Austin, TX) in a three electrode arrangement, with a silver/silver chloride (Ag/AgCl) electrode filled with saturated TBACl in methanol as the reference, platinum foil as the counter and a glassy

carbon electrode (GCE, BAS, 3 mm diameter) as the working electrode. The reference electrode was separated from the working solution by an electrolytic bridge filled with 0.1 M tetrabutylammonium hexafluorophosphate/DMF (TBAHFP/DMF) solution. The reference potential electrode was calibrated by using the ferrocene oxidation process in the same TBAHFP/DMF solution. 0.1 M TBAHFP/DMF was used as the supporting electrolyte solution. Argon was used to deaerate the solution and an argon blanket was maintained over the solution during all experiments. All experiments were carried out at 25 °C. The GC electrode was polished mechanically with 1.0, 0.3 and 0.05 μm alumina powder on a Buehler polishing cloth to a mirror-like surface. Finally, it was rinsed with methanol and sonicated in pure methanol.

Conclusions

Synthesis and properties of the [3]rotaxanes containing tetraazamacrocyclic complexes and two DB24C8 macrocycles per molecule are described. [3]rotaxanes crystallise at a special position (symmetry centre) in $P\bar{1}$ and $P2_1/n$ space groups from the triclinic and monoclinic crystal systems. The positively charged [3]rotaxane moieties form cavities in the crystal lattice which are filled in by disordered anions and solvent molecules. Both [3]rotaxanes have a flexibleaxle. Their shape depends on packing and intra-, and intermolecular interactions among the moieties in the crystal and can be either closer to the "S"-letter or it can be more linear. In both compounds, adjacent dibenzo-24-crown-8 ether wheels are located close to the Ni center of the TAM^{2+} unit in a way that aromatic rings are involved in the Ni···π contacts. The interactions between Ni center and crown rings can be observed by electrochemical means. Incorporation of two crown rings into axle molecules causes steric congestion around the metallic center, hinders the access of counterions, and therefore shifts the oxidation of the metallic center potential toward more positive values.

Conflicts of interest

There are no conflicts to declare.

Acknowledgements

We would like to thank Professor Bohdan Korybut-Daszkiewicz for valuable discussions.

Financial support from the National Science Centre in Poland (NCN, Grant OPUS No. 2014/13/B/ST5/03727) is gratefully acknowledged.

The single-crystal X-ray diffraction analysis was carried out at the Biological and Chemical Research Centre, University of Warsaw, established within the project co-financed by European Union from the European Regional Development Fund under the Operational Programme Innovative Economy, 2007–2013. This research was supported by the 501-D112-86-DSM-115 100 grant (DT – structural analysis) and the data collection was accomplished at the Core Facility for crystallographic and biophysical research to support the development of medicinal products sponsored by the Foundation for Polish Science (FNP).

Notes and references

1 C. J. Bruns and J. F. Stoddart, *The nature of the mechanical bond: from molecules to machines*, Wiley, Hoboken, New Jersey, 2017.
2 J. F. Stoddart, *Angew. Chem., Int. Ed.*, 2017, **56**, 11094.
3 J.-P. Sauvage, *Angew. Chem., Int. Ed.*, 2017, **56**, 11080.
4 R. D. Astumian, *Chem. Sci.*, 2017, **8**, 840.
5 S. Kassem, T. van Leeuwen, A. S. Lubbe, M. R. Wilson, B. L. Feringa and D. A. Leigh, *Chem. Soc. Rev.*, 2017, **46**, 2592.
6 A. J. McConnell, C. S. Wood, P. P. Neelakandan and J. R. Nitschke, *Chem. Rev.*, 2015, **115**, 7729.
7 S. Erbas-Cakmak, D. A. Leigh, C. T. McTernan and A. L. Nussbaumer, *Chem. Rev.*, 2015, **115**, 10081.
8 J. E. M. Lewis, M. Galli and S. M. Goldup, *Chem. Commun.*, 2017, **53**, 298.
9 S. F. M. van Dongen, S. Cantekin, J. A. A. W. Elemans, A. E. Rowan and R. J. M. Nolte, *Chem. Soc. Rev.*, 2014, **43**, 99.
10 B. L. Feringa, *Angew. Chem., Int. Ed.*, 2017, **56**, 11060.
11 B. Korybut-Daszkiewicz, A. Wieckowska, R. Bilewicz, S. Domagała and K. Woźniak, *Angew. Chem., Int. Ed.*, 2004, **43**, 1668.
12 B. Korybut-Daszkiewicz, A. Więckowska, R. Bilewicz, S. Domagała and K. Woźniak, *J. Am. Chem. Soc.*, 2001, **123**, 9356.
13 I. Mames, J. Kowalski, P. Świder and B. Korybut-Daszkiewicz, *Chem. Heterocycl. Compd.*, 2017, **53**, 87.
14 M. Woźny, J. Pawłowska, A. Osior, P. Świder, R. Bilewicz and B. Korybut-Daszkiewicz, *Chem. Sci.*, 2014, **5**, 2836.
15 M. Woźny, J. Pawłowska, K. M. Tomczyk, R. Bilewicz and B. Korybut-Daszkiewicz, *Chem. Commun.*, 2014, **50**, 13718.
16 K. M. Tomczyk, M. Woźny, S. Domagała, A. Więckowska, J. Pawłowska, K. Woźniak and B. Korybut-Daszkiewicz, *New J. Chem.*, 2017, **41**, 6004.
17 B. Korybut-Daszkiewicz, R. Bilewicz and K. Woźniak, *Coord. Chem. Rev.*, 2010, **254**, 1637.
18 S. Garaudée, S. Silvi, M. Venturi, A. Credi, A. H. Flood and J. F. Stoddart, *ChemPhysChem*, 2005, **6**, 2145.
19 A. B. Braunschweig, C. M. Ronconi, J.-Y. Han, F. Aricó, S. J. Cantrill, J. F. Stoddart, S. I. Khan, A. J. P. White and D. J. Williams, *Eur. J. Org. Chem.*, 2006, 1857.
20 S. J. Loeb and J. A. Wisner, *Angew. Chem., Int. Ed.*, 1998, **37**, 2838.
21 S. J. Loeb and J. A. Wisner, *Chem. Commun.*, 1998, 2757.
22 D. J. Mercer and S. J. Loeb, *Dalton Trans.*, 2011, **40**, 6385.
23 D. J. Mercer, S. J. Vella, L. Guertin, N. D. Suhan, J. Tiburcio, V. N. Vukotic, J. A. Wisner and S. J. Loeb, *Eur. J. Org. Chem.*, 2011, 1763.
24 K. Zhu, V. N. Vukotic and S. J. Loeb, *Chem. – Asian J.*, 2016, **11**, 3258.

25 N. Farahani, K. Zhu and S. J. Loeb, *ChemPhysChem*, 2016, **17**, 1875.
26 K. Zhu, V. N. Vukotic, N. Noujeim and S. J. Loeb, *Chem. Sci.*, 2012, **3**, 3265.
27 D. Thibeault and J.-F. Morin, *Molecules*, 2010, **15**, 3709.
28 V. Aucagne, J. Berná, J. D. Crowley, S. M. Goldup, K. D. Hänni, D. A. Leigh, P. J. Lusby, V. E. Ronaldson, A. M. Z. Slawin, A. Viterisi and D. B. Walker, *J. Am. Chem. Soc.*, 2007, **129**, 11950.
29 B. K. Juluri, A. S. Kumar, Y. Liu, T. Ye, Y.-W. Yang, A. H. Flood, L. Fang, J. F. Stoddart, P. S. Weiss and T. J. Huang, *ACS Nano*, 2009, **3**, 291.
30 A. N. Basuray, H.-P. Jacquot de Rouville, K. J. Hartlieb, T. Kikuchi, N. L. Strutt, C. J. Bruns, M. W. Ambrogio, A.-J. Avestro, S. T. Schneebeli, A. C. Fahrenbach and J. F. Stoddart, *Angew. Chem., Int. Ed.*, 2012, **51**, 11872.
31 S. Lee, C.-H. Chen and A. H. Flood, *Nat. Chem.*, 2013, **5**, 704.
32 N. S. Simpkins, D. F. Weske, L. Male, S. J. Coles and M. B. Pitak, *Chem. Commun.*, 2013, **49**, 5010.
33 E. A. Neal and S. M. Goldup, *Chem. Sci.*, 2015, **6**, 2398.
34 A. G. Kolchinski, R. A. Roesner, D. H. Busch and N. W. Alcock, *Chem. Commun.*, 1998, 1437.
35 S. J. Loeb and J. A. Wisner, *Chem. Commun.*, 2000, 845.
36 Y. Furusho, T. Hasegawa, A. Tsuboi, N. Kihara and T. Takata, *Chem. Lett.*, 2000, **29**, 18.
37 S.-H. Chiu, A. M. Elizarov, P. T. Glink and J. F. Stoddart, *Org. Lett.*, 2002, **4**, 3561.
38 W. Jiang, H. D. F. Winkler and C. A. Schalley, *J. Am. Chem. Soc.*, 2008, **130**, 13852.
39 M. A. Soto and J. Tiburcio, *Chem. Commun.*, 2016, **52**, 14149.
40 J. Sawada, D. Aoki, S. Uchida, H. Otsuka and T. Takata, *ACS Macro Lett.*, 2015, **4**, 598.
41 T. Ogawa, K. Nakazono, D. Aoki, S. Uchida and T. Takata, *ACS Macro Lett.*, 2015, **4**, 343.
42 D. Aoki, S. Uchida and T. Takata, *Angew. Chem., Int. Ed.*, 2015, **54**, 6770.
43 Z. Meng and C.-F. Chen, *Org. Biomol. Chem.*, 2014, **12**, 6937.
44 Z. Zhang, C. Han, G. Yu and F. Huang, *Chem. Sci.*, 2012, **3**, 3026.
45 M. Woźny, *Synthesis*, 2018, DOI: 10.1055/s-0037-1609915.
46 *CrysAlis CCD and CrysAlis RED, Oxford Diffraction*, Oxford Diffraction Ltd, Yarnton, 2008.
47 R. C. Clark and J. S. Reid, *Acta Crystallogr., Sect. A: Fundam. Crystallogr.*, 1994, **51**, 887.
48 G. M. Sheldrick, *Acta Crystallogr., Sect. A: Fundam. Crystallogr.*, 2008, **64**, 112.
49 (*a*) O. V. Dolomanov, L. J. Bourhis, R. J. Gildea, J. A. K. Howard and H. Puschmann, *J. Appl. Crystallogr.*, 2009, **42**, 339; (*b*) C. F. Macrae, P. R. Edgington, P. McCabe, E. Pidcock, G. P. Shields, R. Taylor, M. Towler and J. van de Streek, *J. Appl. Crystallogr.*, 2006, **39**, 453.
50 A. L. Spek, *Acta Crystallogr., Sect. D: Biol. Crystallogr.*, 2009, **65**, 148.